scientific reports

OPEN

Recycling of zinc ions in disc-donut column considering forward mixing mass transfer, and effects of pulsed and non-pulsed condition

Mehdi Asadollahzadeh[1✉], Rezvan Torkaman[1], Meisam Torab-Mostaedi[1] & Mojtaba Saremi[2]

The current study focuses on the recovery of zinc ions by solvent extraction in the pulsed contactor. The Zn(II) ions from chloride solution were extracted into the organic phase containing di-(2-ethylhexyl) phosphoric acid (D2EHPA) extractant. The resulting data were characterized for the relative amount of (a) pulsed and no-pulsed condition; and (b) flow rate of both phases. Based on the mass balance equations for the column performance description, numerical computations of mass transfer in a disc-donut column were conducted and validated the experimental data for zinc extraction. Four different models, such as plug flow, backflow, axial dispersion, and forward mixing were evaluated in this study. The results showed that the intensification of the process with the pulsed condition increased and achieved higher mass transfer rates. The forward mixing model findings based on the curve fitting approach validated well with the experimental data. The results showed that an increase in pulsation intensity, as well as the phase flow rates, have a positive impact on the performance of the extractor. In contrast, the enhancement of flow rate led to the reduction of the described model parameters for the adverse phase.

List of Symbols

Af — Pulse intensity (cm/s)
a — Specific surface area per unit volume ($6\varphi/d_{32}$) (1/m)
d — Drop diameter (m or mm)
d_{32} — Sauter mean drop diameter (mm)
d_{43} — Mean diameter (m)
E — Axial dispersion coefficient (cm^2/s)
f — Volumetric drops size distribution (–)
g — Dynamic drop size distribution (–)
H — Height of column (m)
K — Overall mass transfer coefficient (m/s)
n — Number of drops (–)
N_d — Number of drop classes (–)
P — Drop size distribution
Q — Volume flow rate (L/h)
S — Cross-section area of the column (m^2)
t — Residence time of drops (s)
u — Drop velocity (m/s)
U — Superficial velocity (Q/S) (m/s)
U_{slip} — Slip velocity ($U_c/(1-\varphi) + U_d/\varphi$) (m/s)
V — Volume of phases (m^3)
x — Mass fraction of solute in the continuous phase (–)
y — Mass fraction of solute in the dispersed phase (–)
z — Height variable (m

[1]Nuclear Fuel Cycle Research School, Nuclear Science and Technology Research Institute, P.O. Box: 11365-8486, Tehran, Iran. [2]Energy Engineering and Physics Department, Amirkabir University of Technology, P.O. Box: 15875-4413, Tehran, Iran. ✉email: masadollahzadeh@aeoi.org.ir

Dimensionless symbols

NTU	Number of transfer unit ($K_{od}aH/U_d$)
p	Slope of the concentration equilibrium equation ($y = p^*x + q$)
Pe	Peclet number (HU/E)
q	Constant of the concentration equilibrium equation ($y = p^*x + q$)
X	Continuous phase concentration (($\mathbf{x} - \mathbf{x}^*_{out}$)/($x_{in} - x^*_{out}$))
Y	Dispersed phase concentration (($y - y_{in}$)/($y^*_{out} - y_{in}$))
Z	Height ($Z = z/H$)
Ω	Constant ($pU_d\rho_d/U_c\rho_c$

Greek symbols

α	Continuous phase backflow coefficient (–)
β	Dispersed phase backflow coefficient (–)
μ	Viscosity (kg/m.s)
ρ	Density (kg/m^3)
σ	Interfacial tension between two phases (N/m)
φ	Dispersed phase holdup (–

Subscripts/superscripts

$*$	Equilibrium concentration
c	Continuous phase
d	Dispersed phase
i	Drop class
in	Inlet to the column
j	Cross-section
out	Outlet from the column
AARE	Average Absolute Relative Error
ADM	Axial Dispersion Model
BFM	Back Flow Model
PFM	Plug Flow Model
FMM	Forward Mixing Model

Abbreviations

AARE	Average Absolute Relative Error
ADM	Axial Dispersion Model
BFM	Back Flow Model
PFM	Plug Flow Model
FMM	Forward Mixing Model

The find of many applications in various extraction processes such as chemical, and petroleum industries is one of the main advantages of pulsed solvent extraction columns[1,2]. The main specific characteristic of this column is the utilization of pulsing conditions for the intensified process; it is possible not only to increase its efficiency; but also to obtain compactness of equipment, to diminish maintenance efforts, and to improve the quality of extracted products[3–5]. However, these columns have grown well in the extraction stages from a primary source such as the leaching aqueous solution[6–9]. But, its path to secondary resource development and recovery has slowed in industries. Recovery of toxic metals from wastewaters is one of the needs of environmental refinement done by various processes[10–14]. The use of the solvent extraction process has expanded with environmentally friendly solvents[15,16]. But the solvent type alone is not enough to achieve the desirability, and the selected equipment must have a good performance[17].

Zinc is one of the heavy metals with adverse effects on water resources, soils, vegetables, and crops[18]. In some areas, this pollution is hazardous to human health[19]. The extraction and separation of which is critical from an environmental point of view. Jafari and co-workers' studies showed that zinc could be extracted from a synthetic solution with a high extraction percentage ~ 94% with D2EHPA extractant[20]. The zinc recovery process from effluents such as spent chloride brass pickle liquors[21], and zinc-plating mud[22] has been investigated in the literature. Extraction species depend on different acidic conditions and type of extractant (D2EHPA, Bis(2,4,4-trimethylpentyl) dithiophosphinic Acid (Cyanex301), bis/2,4,4-trimethylpentyl/ phosphinic acid (Cyanex272), 5-nonylacetophenona oxime (LIX 84IC)), and ionic liquids. The zinc recovery from the complex ore resources was investigated by a mixture of trioctylphosphine oxide (TOPO) and tricaprylylmethylammonium chloride (Aliquate336) in the extraction stage and the ammoniacal chloride solution in the stripping stage.

Zinc metal extraction depends on various factors such as the concentration of the extractant, the acidity of the solution and other impurities in the solution. Therefore, extraction is limited by the presence of contaminants. Still, the distribution coefficients of zinc in the phosphoric extractant are high and it is transferred to the organic phase with a higher distribution ratio than other ions such as cobalt and manganese. Also, the operating conditions in the extraction columns is very important. The higher extraction efficiency is carried out in a column with proper mixing of droplets in continuous phase under agitation or pulsation condition. This mixing creates an interfacial area which is the main factor in the mass transfer between the two phases.

Model	Governing equations	Remarks	Assumptions
PFM	$\frac{dX}{dZ} + \Omega NTU_{od}(X - Y) = 0$	Continuous phase mass balance	The assumptions of this model are pure plug flow, no axial mixing, equal diameter, velocity, residence time and mass transfer rate for all droplets, the constant of mass transfer coefficient for all droplets, no breakage and coalescence of drops
	$\frac{dY}{dZ} + NTU_{od}(X - Y) = 0$	Dispersed phase mass balance	
	$Z = 0 \rightarrow X^0 = X^{in} = 1$	Boundary Conditions at top of column (z = 0)	
	$Z = 1 \rightarrow Y^1 = Y^{in} = 0$	Boundary Conditions at bottom of column (z = H)	
BFM	$(1 + \alpha)X_{n-1} - (1 + 2\alpha)X_n + \alpha X_{n+1} - \frac{\Omega NTU_{od}}{N}(X_n - Y_n) = 0$	Continuous phase mass balance	The assumptions of this model are pure plug flow with axial mixing, an axial mixing with backflow coefficients of α and β, equal values for diameter, velocity, residence time and mass transfer rate of droplets, no breakage and coalescence of drops
	$(1 + \beta)Y_{n+1} - (1 + 2\beta)Y_n + \beta Y_{n-1} + \frac{NTU_{od}}{N}(X_n - Y_n) = 0$	Dispersed phase mass balance	
	$Z = 0 \rightarrow \begin{cases} X_0 + \alpha(X_0 - X_1) = 1 \\ Y^0 = Y_0 = Y_1 \end{cases}$	Boundary Conditions at top of column (z = 0)	
	$Z = 1 \rightarrow \begin{cases} X^{N+1} = X_{N+1} = X_N \\ Y_{N+1} - \beta(Y_N - Y_{N+1}) = 0 \end{cases}$	Boundary Conditions at bottom of column (z = H)	
ADM	$\frac{dX}{dZ} - \frac{1}{Pe_c}\frac{d^2X}{dZ^2} + \Omega NTU_{od}(X - Y) = 0$	Continuous phase mass balance	The assumptions of this model are pure plug flow with axial mixing, a diffusion process with the constant diffusion coefficients of E_c and E_d, equal values for diameter, velocity, residence time and mass transfer rate of droplets, no breakage and coalescence of drops
	$\frac{dY}{dZ} + \frac{1}{Pe_d}\frac{d^2Y}{dZ^2} + NTU_{od}(X - Y) = 0$	Dispersed phase mass balance	
	$Z = 0 \rightarrow \begin{cases} \left(\frac{U_c}{E_c}\right)(1 - X^0) = -\frac{dX}{dZ}\big|_0 \\ \frac{dY}{dZ}\big|_0 = 0 \rightarrow Y^0 = Y^{out} \end{cases}$	Boundary Conditions at top of column (z = 0)	
	$Z = 1 \rightarrow \begin{cases} \frac{dX}{dZ}\big|_1 = 0 \rightarrow X^1 = X^{out} \\ \left(\frac{U_d}{E_d}\right)(Y^1) = -\frac{dX}{dZ}\big|_1 \end{cases}$	Boundary Conditions at bottom of column (z = H)	
FMM	$\frac{dX}{dZ} - \frac{1}{Pe_c}\frac{d^2X}{dZ^2} + \Omega \sum_{i=1}^{N} NTU_{od,i}(X - Y_i) = 0$	Continuous phase mass balance	The main assumptions of this model are the constant values of inlet and outlet flow rates, the use of the axial dispersion coefficient (E_c) for the deviation of the continuous phase from the plug state, no coalescence and breakage of dispersed phase droplets
	$\frac{dY_i}{dZ} + \frac{NTU_{od,i}}{g_i}(X - Y_i) = 0 \ (i = 1, 2, \ldots N)$	Dispersed phase mass balance	
	$Z = 0 \rightarrow \begin{cases} \left(\frac{U_c}{E_c}\right)(1 - X^0) = -\frac{dX}{dZ}\big|_0 \\ Y_i^0 = Y_i^{out} (i = 1, 2, \ldots N) \end{cases}$	Boundary Conditions at top of column (z = 0)	
	$Z = 1 \rightarrow \begin{cases} \frac{dX}{dZ}\big|_1 = 0 \rightarrow X^1 = X^{out} \\ Y_i^1 = Y^{in} = 0 (i = 1, 2, \ldots N) \end{cases}$	Boundary Conditions at bottom of column (z = H)	
	$g_i = \frac{f_i u_i}{\sum_{j=1}^{N} f_j u_j}$	Dynamic drop size distribution	
	$u_i = \frac{d_i}{d_{43}} U_{slip} - \frac{U_c}{1-\phi}$	Drop velocity	
	$d_{43} = \sum_{i=1}^{N} \frac{n_i d_i^4}{\sum_{j=1}^{N} n_j d_j^3}$		
	$f_i = \frac{P_i^3}{\sum_{i=1}^{N} P_i^3}$	Volumetric drop size distribution	
	$a_i = \frac{6\phi_i}{d_i}$	Drop specific surface area	
	$\phi_i = \phi f_i$	Drop holdup	

Table 1. Mass balance equations for four models[31].

The synergistic effects in the extraction stage and the antagonistic effects in the stripping stage are the advantages of using a mixture of extractants[23]. The melting effluents are rich sources of heavy metals such as zinc, copper, nickel, and cadmium. Studies on the recovery of these ions with 2-hydroxy-5-nonylacetophenone oxime and Cyanex272 have shown that the solvent extraction process can play an influential role in their recovery and reduce environmental impact[24]. The technology for extracting zinc from molten effluents has been extensively developed, but the issue of removing other ions has received little research. Song and co-workers reported the extraction of cobalt ions from these effluents for recovery due to the value of cobalt in various industries[25].

In addition to experimental work, it is possible to describe the process based on different models and mass transfer coefficients[26–30]. The mass balance induced by rising droplets or continuous phase can be crucial in the numerical modeling of the extraction column[31]. Using the mathematical models of the extraction process, it is possible to deduce the dependences of the mass transfer coefficient on the operating condition, and the dependence of the mass transfer coefficient on the physical properties[32,33]. The evaluation of concentration profile curves is of paramount importance, especially for establishing the optimum operating conditions, determining parameters used for scale-up and process design. Mathematical modeling of the extraction column is fundamental due to the economic potential[34]. It is important to develop models for the process to optimize the extraction operation for commercial applications. However, such predictions require establishing a model predicting column performance[35,36]. The plug flow model (PFM) is common with simple assumptions in determining mass transfer coefficients. The backflow model (BFM) and axial dispersion model (ADM) are described by determining the specific coefficients for the deviation from the ideal state[31]. The forward mixing model (FMM) is more superior
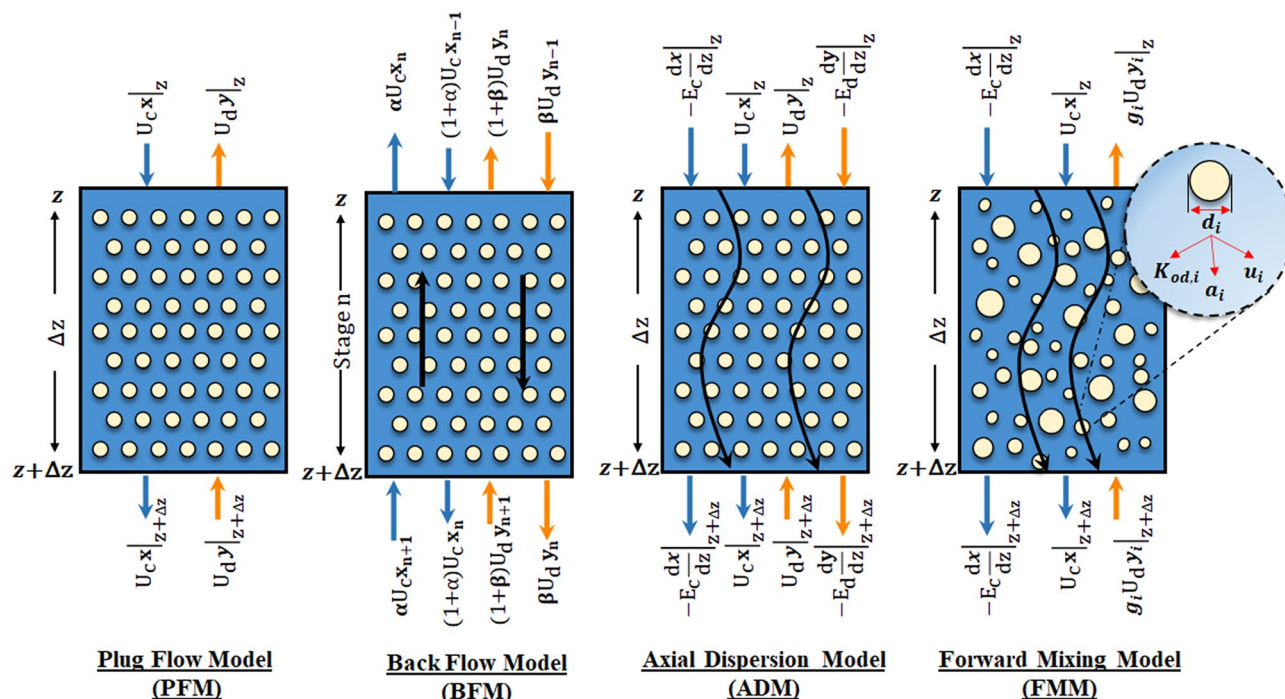
Figure 1. Mass balance over a volumetric element based on the plug flow, back-flow, axial dispersion and forward mixing models.

Phases								Σ (10^{-3} N/m)
continuous	Dispersed	Solute	ρ_c (kg/m³)	ρ_d (kg/m³)	μ_c (10^{-3} kg/m s)	μ_d (10^{-3} kg/m s)		
Aqueous nitrate solution of Zn(II)	D2EHPA extractant diluted in kerosene	Zinc ions	1011	824	0.975	1.615		18.7

Table 2. Characteristics of chemical system used in the pilot-plant column.

to the three mentioned models. Applying droplet size distribution in the model helps bring the extraction conditions closer to the actual conditions[37,38]. The exchange of mass transfer between the aqueous and organic phases takes place in the interface of two phases. Interfacial tension significantly affects the droplet size distribution and the required zone for mass transfer. Therefore, the interface of both phases and the creation of different mass transfer phenomena between droplets are very effective in increasing the mass transfer coefficients. Also, interfacial energy dominates over the volume force with considerable surface to volume ratio in micro scale. This phenomenon leads to distinct behavior from those of the macroscopic systems[39].

Mass balance equations illustrate these models, these equations are described in Table 1, and a schematic of the mass transfer equilibrium based on the PFM, BFM, ADM, and FMM models is given in Fig. 1.

Several physical systems have been investigated in the pilot-scale pulsed disc-donut column in the literature[40–43], but limited studies have been reported with this column to extract metal ions associated with the reaction condition[4,44–46]. One of the new findings and innovations of this paper is the study of different mass transfer models in the extraction of zinc ions. So far, no studies have been reported in this field, and this finding is significant in the design of this pulsed column according to the standard chemical system for zinc extraction.

Experimental

Materials. A series of continuous experiments were carried out to remove zinc ions from an aqueous solution at room temperature (25 ± 1.5 °C). The extraction process was carried out by preparing two aqueous and organic solutions. The organic solution was obtained from the dissolution of an extractant from Aldrich company, di-(2-ethylhexyl) phosphoric acid/ D2EHPA (0.1 M) in kerosene. The aqueous solution was obtained from the dissolution of zinc chloride salt (Merck Company, with 99% purity) in distilled water with a concentration equivalent to 600 ppm at pH ~ 6. The details of physical properties are shown in Table 2.

Pilot plant column. As shown in Fig. 2, the experiments have been carried out in a 0.076 m diameter disc-donut column with a 0.74 m long glass extraction section. The average fractional free area has been maintained at 23.5%. The arrangement of discs and donuts inside the column was made so that 30 discs (0.067 cm O.D) and donuts (0.036 cm I.D) were placed one by one inside the active part.
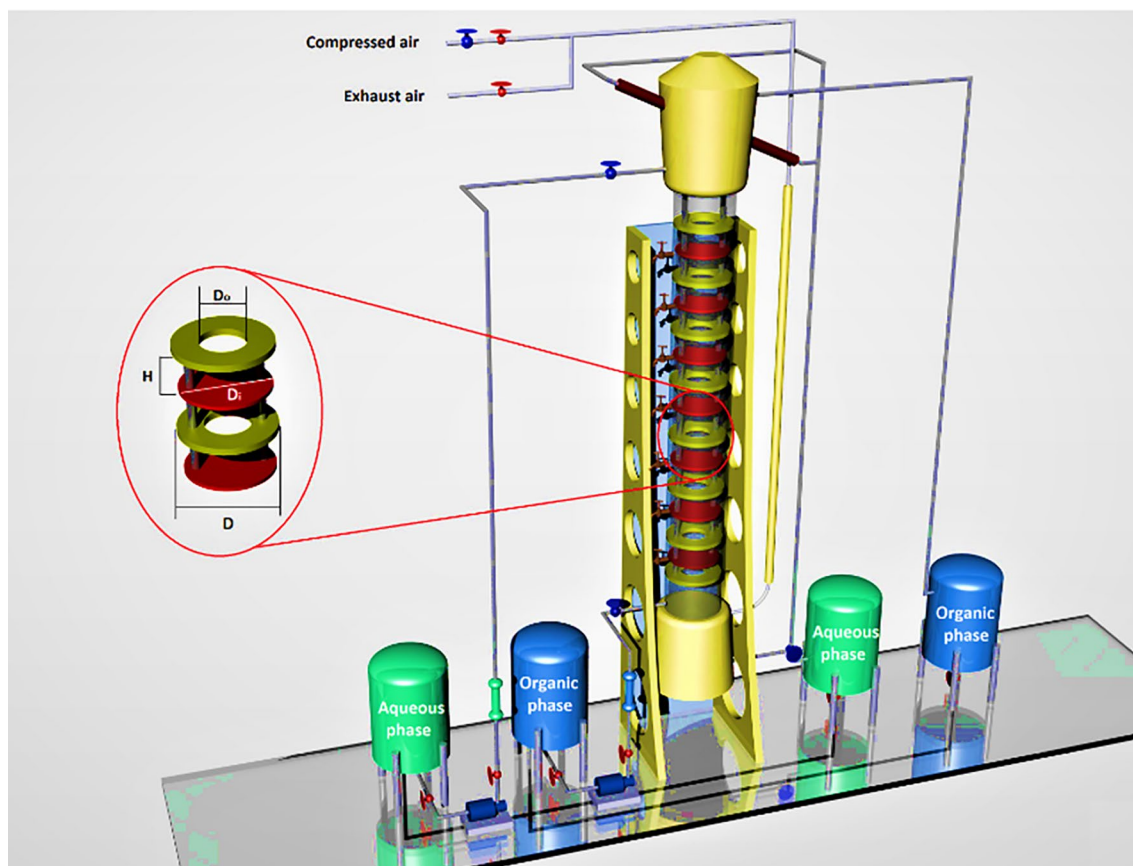
Figure 2. Schematic view of a pilot plant pulsed disc-donut column.

	PFM		BFM		ADM		FMM	
Conditions	**AAREX (%)**	**AAREY (%)**	**AAREX (%)**	**AAREY (%)**	**AAREX (%)**	**AAREY (%)**	**AAREX (%)**	**AAREY (%)**
Without pulsation	10.93	38.63	5.76	22.35	3.92	11.37	2.38	7.87
With pulsation	13.66	22.48	11.44	17.12	12.88	16.37	10.74	13.28

Table 3. Comparison of the AARE values between PFM, BFM, ADM, and FMM models.

The aqueous and organic phases are pumped into the column from two stainless steel tanks and the control of flows with two rotameters. The photos of droplets in the column were recorded by a video camera, installed at the center of the column section. The evaluation of drop sizes was obtained by the Sauter mean drop size (d_{32}) values for each run. The composition of the aqueous solution in the feed and residual was determined by using UV-spectrophotometer (UNICO model). The shutdown method was used to measure the value of holdup (φ) from the separation of the organic phase in the interface location. The interfacial area for the reaction between zinc ions and extractants in the organic phase was obtained by the following equation:

$$a = \frac{6\varphi}{d_{32}} \tag{1}$$

The mass transfer coefficient for the organic-side phase was calculated using four models (PFM, BFM, ADM, and FMM models) in Table 1.

Results and discussion

The zinc extraction process in the pulsed disc-donut column was continuously investigated in two steps. In the first step, the pulse conditions inside this column were not activated, and only the effects of phase flow rates were investigated in this column. In the second step, pulse conditions were applied inside the column. Different intensities of the pulse were investigated, and the variation in the phase flow rates at different pulse intensities was studied in this column. Four different types of models (PFM, BFM, ADM, FMM models) were evaluated in the performance recognition of this column, according to Table 1. The model analysis result showed that the
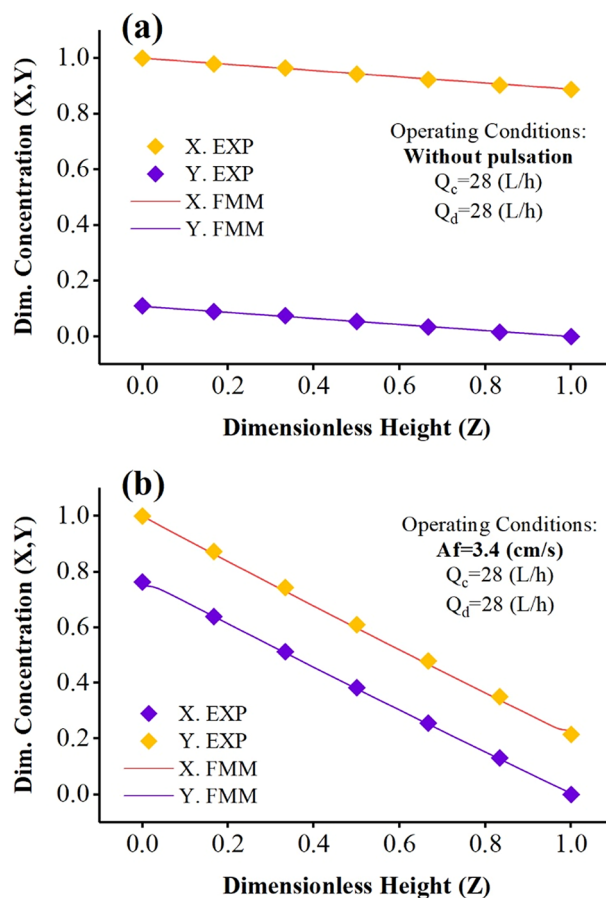
Figure 3. Comparison of laboratory concentration profiles with predicted by the forward mixing model under $Q_c = Q_d = 28$ (L/h) and (**a**) without pulsation, (**b**) Af = 3.4 (cm/s).

column behavior using the FMM model is closer to the real values. The errors from the experimental data are much less with the FMM model results. The variation in X-valve and Y-value errors with average absolute relative error (AARE) are presented in Table 3, which indicates that the pulsed disc-donut column is more consistent with the forward mixing model (10.74% for X-value, 13.28% for Y-value).

The main reason for reducing errors is related to the distribution of droplets inside the column, which applies the droplet distribution in the forward model and avoids simplifying assumptions that bring the column's behavior closer to the actual value. Table 3 shows the plug flow model with simple assumptions is associated with more errors. The backflow and axial mixing models are related to significant errors that are acceptable to use in the study of column behavior. The back-mixing and axial dispersion coefficients defined in these models help the system approach the ideal conditions.

Figures 3 and 4 show the examples of concentration profiles measured by the experimental method under different operating conditions and the concentration profiles predicted by the forward mixing model to extract zinc ions.

The results in this diagram showed that without applying a pulse inside the column, a large mass transfer driving force is established in the column that cannot reach the desired mass transfer and efficiency (see Fig. 3a). But when the pulse is applied inside the column, the column conditions lead to better mass transfer and intensification of the process, which reduces the driving force of the mass transfer is shown in Fig. 3b.

Increasing the continuous phase flow rates in Figs. 3b, 4a, b, increasing the phase flow ratio (Q_c/Q_d) causes a change in the mass transfer's driving force. The decrease in driving force indicates that the phase change curves of the phases are getting closer to each other. The system is closer to ideal conditions and optimal extraction. Therefore, creating pulse conditions and increasing the inlet aqueous phase flow rates intensify the process and reach equilibrium concentrations. Another finding in these two graphs is the correspondence between the forward model and the laboratory data, which shows that the descriptive model can be used with high accuracy in predicting the results.

The changes in backflow coefficients for aqueous and organic-side phases are shown in Figs. 5, and 6 by examining the effect of operating parameters. These figures showed that increasing the pulse intensity inside the column leads to increasing the back-flow coefficients. Further stress due to the pulse causes the increase in collision frequency of the droplet with the column's internal components. This factor increases the backflow coefficients (α, and β).
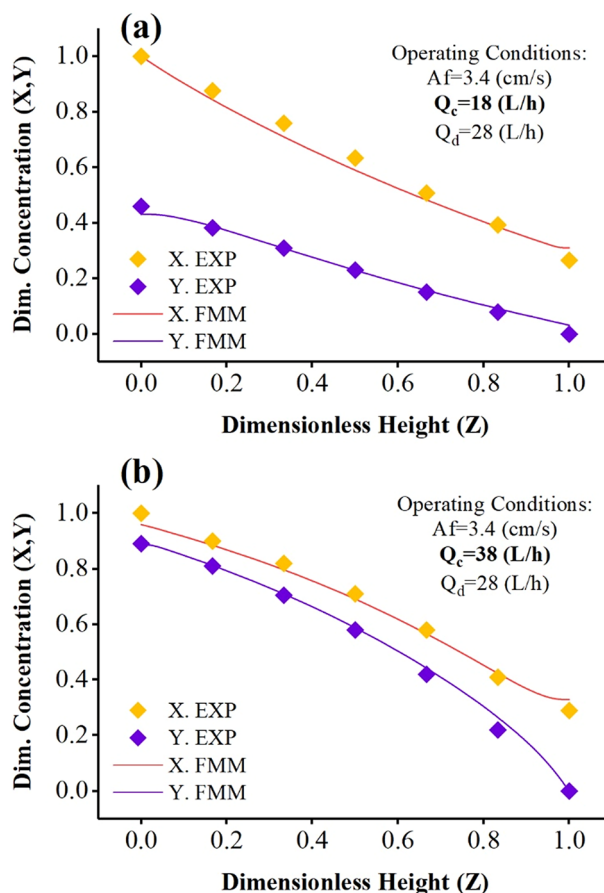
Figure 4. Comparison of laboratory concentration profiles with predicted by the forward mixing model under $Q_d = 28$ (L/h) and $Af = 3.4$ (cm/s) and (**a**) $Q_c = 18$ and (**b**) $Q_c = 38$ (L/h).

The effect of increasing the continuous phase flow rate on the α, and β coefficients showed that increasing of Q_c increases the frequency of collisions with the internal parts, increasing the aqueous-side phase coefficients (α). But it adversely affects on the organic side-phase coefficients (β), because the higher continuous flow rate helps carry droplets. Increasing the dispersed phase flow rate also reduces α and increases β coefficients. Because with the presence of more droplets inside the column, the coalescence rate increases, which has the opposite effect on the α coefficient, but also helps increase the number of collisions at a constant volume for a higher number of droplets and increase the β coefficient.

The results showed that the lack of pulse inside the column is associated with an increase in these coefficients and increases the deflection conditions of the plug flow. However, the use of pulses inside the column causes the necessary stresses to provide a better flow, which intensifies the column's process and better performance by describing the mass transfer coefficients.

The results in Fig. 7 described that increasing the pulse intensity at constant phase flow rates increases the axial dispersion coefficient for the aqueous side-phase. With increasing turbulence in the system, the droplet aggregation and the vortex formation increase in a continuous phase. Therefore, the higher values for E_c are observed with an increment of Af.

The variations in the dispersed and continuous phase flow on the axial dispersion coefficient of the continuous phase are shown in Figs. 8 and 9. The increase in Q_c reveals a positive effect, and the increase in Q_d reveals a negative effect on the E_c. The decrement impact is due to uniform conditions with a reduction in collision frequency of droplets with the internal components. The incremental impact is due to the presence of droplets and participation in more turbulence through the column. These coefficients are much larger in non-pulsed conditions, where the deviations from the ideal current are much larger, and the driving force for mass transfer is high, and reaching the perfect conditions is not achieved by changing the phase flow rate alone.

The axial dispersion coefficients for the organic-side phase also change similar to continuous axial dispersion coefficients with operating parameters, as shown in Fig. 10. The increase of this parameter is observed by the pulse intensity in Fig. 10a, c. Its decrease is observed by Q_c in Fig. 10b. Changes in the droplet's behavior inside the column under operating parameters help to significantly affect these coefficients, and the variation in flow deflection becomes apparent.

Mass transfer coefficients were evaluated by the forward mixing model, the results of which are shown in Fig. 11. The observation indicated that as the pulse intensity increases, the droplet diameter decreases, and the dispersed phase holdup increases, increasing the effective interfacial area for the reaction. The reduction in
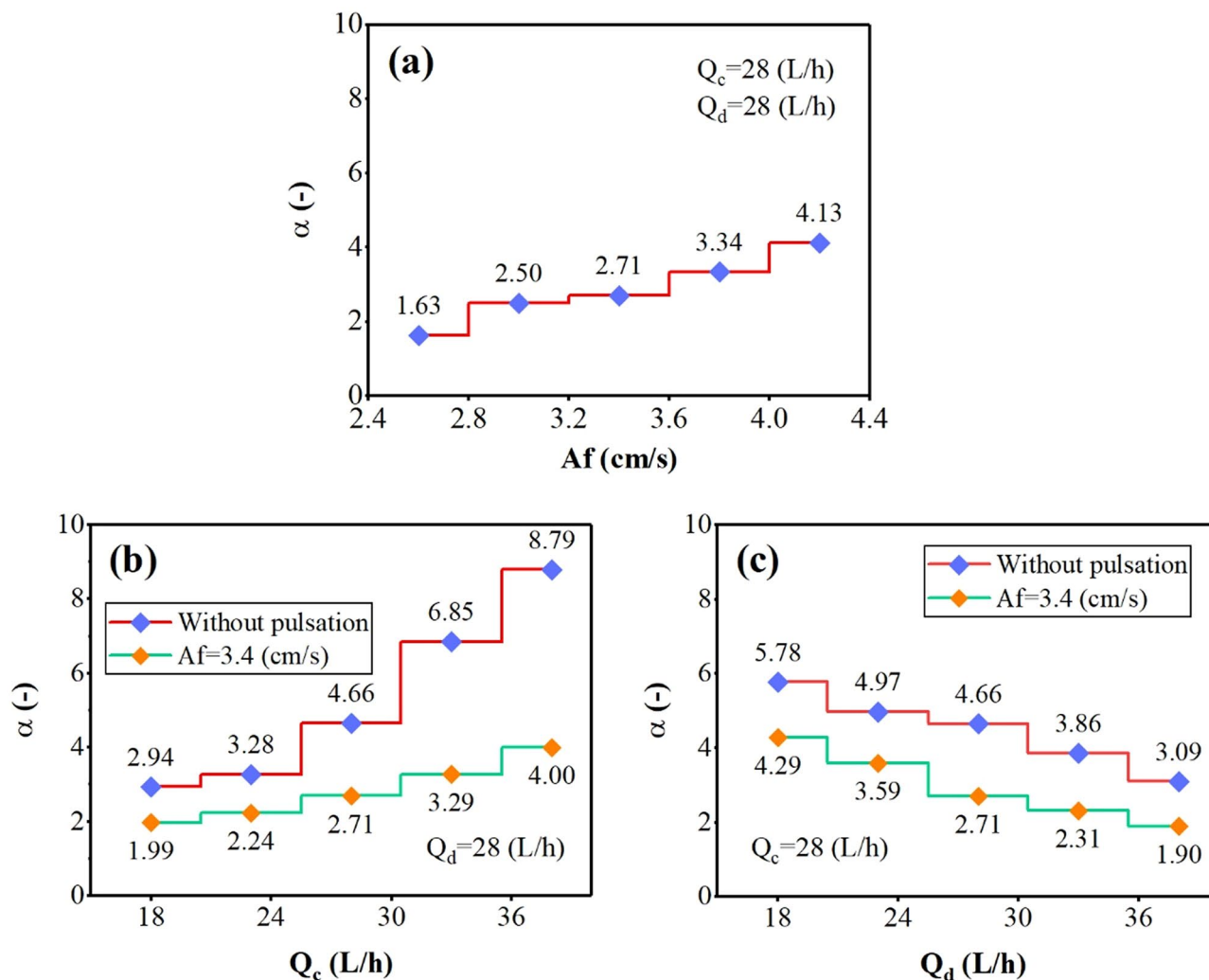
Figure 5. The effect of operating parameters [(**a**) pulsation intensity, (**b**) aqueous phase flow rate, and (**c**) organic phase flow rate] on the continuous phase backflow coefficient.

mass transfer occurs due to the droplet behavior approaching the rigid state and reducing droplet sizes. But the conditions with increasing the required area for the reaction help provide larger volumetric overall mass transfer coefficients. Increasing the phases' flow rate helps to shift the mass transfer rates within the droplets toward the internal circulation, as larger droplets are formed when the coalescence rate increases. In addition to increasing the required interfacial area for the reaction, the mass transfer coefficients for the organic-side phase increase along this column. The results in these figures showed that the pulse conditions are an essential factor in intensifying the column process and providing the requirements for mass transfer. Without this factor inside the column, very small mass transfer coefficients are obtained, indicating the column's poor performance in non-pulsed conditions.

The results of the percentage of zinc extraction with Q_c and Q_d are shown in Fig. 12. The results illustrated that the zinc ions' extraction is a function of the inlet phase rates and pulsed conditions. Increasing the flow rate of the phases helps to establish the higher mass transfer rate in the pulsed disc-donut column and the result is an increase in the percentage of extraction of zinc ions from the aqueous to the organic phase. These diagrams also observe the intensification of the process by applying pulses in the column and performing the extraction reaction, and increasing the efficiency.

The results showed that the disc-donut column could be used to remove and recover heavy metals from effluents. The presence of a pulsing condition inside the column provides a higher interfacial area with better mixing, which results in higher mass transfer and higher operating efficiency. Therefore, pulsed disc-donut columns are very desirable and efficient in reaction conditions.

Conclusion

In this study, the extraction of zinc ions from the aqueous to the organic solution was investigated as a standard reaction system in the pulsed disc-donut column. The operating conditions of the pilot plant column were checked by changing the flow rate of the inlet phases and applying pulses inside the column. The extraction process description was examined the mass transfer models (plug flow, backflow, axial dispersion, and forward
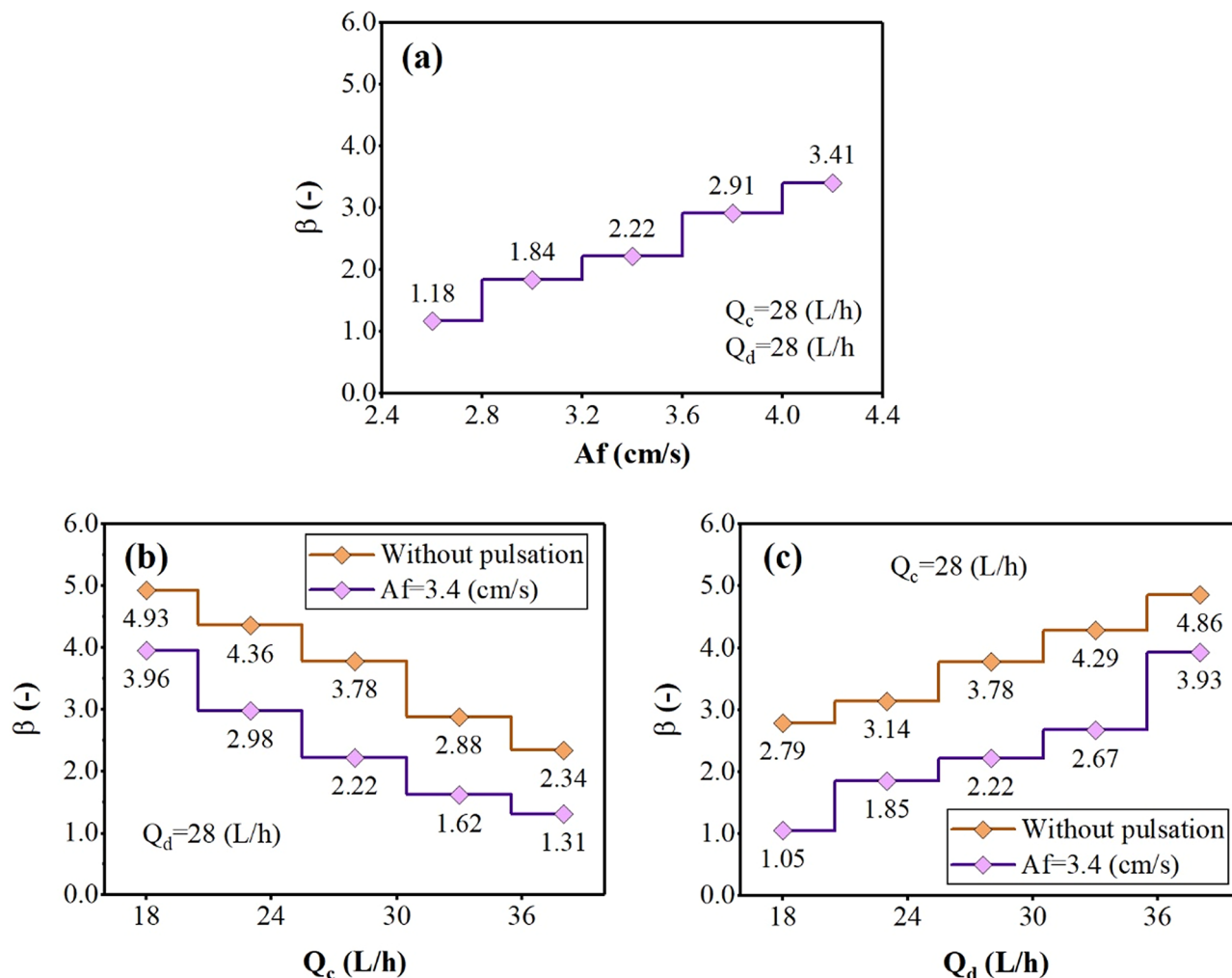
Figure 6. The effect of operating parameters [(**a**) pulsation intensity, (**b**) aqueous phase flow rate, and (**c**) organic phase flow rate] on the dispersed phase backflow coefficient.
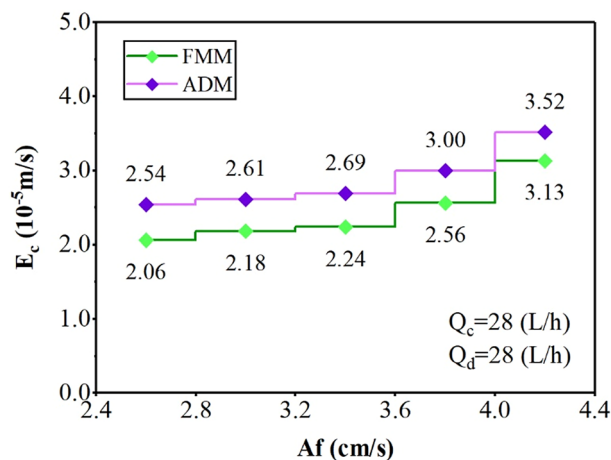

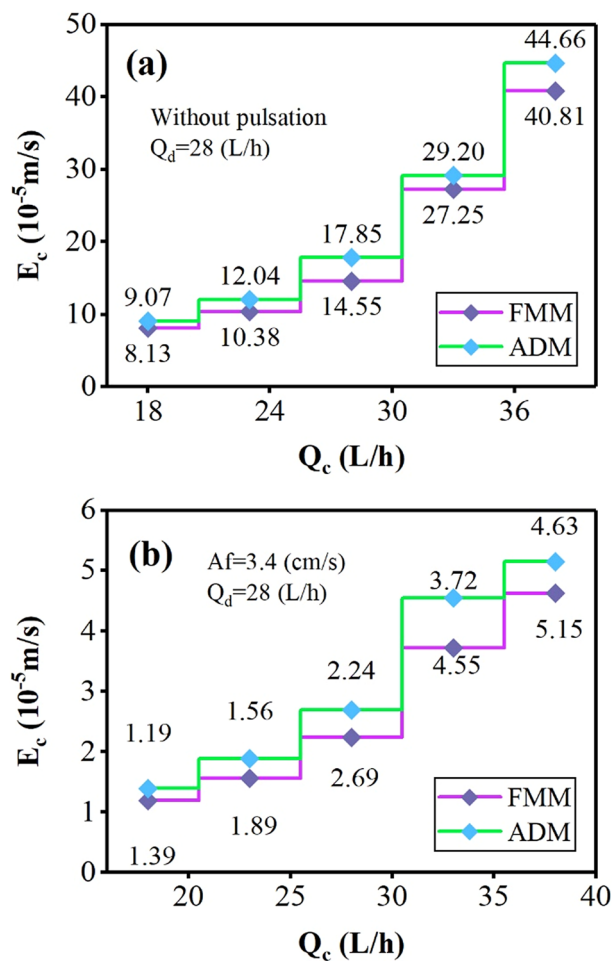**Figure 7.** The effect of pulsation intensity on the continuous phase axial dispersion coefficient.

Figure 8. The effect of aqueous phase flow rate on the continuous phase axial dispersion coefficient (**a**) without pulsation, (**b**) Af = 3.4 (cm/s).

mixing models). The results of variation in the operating parameters showed that the optimal extraction conditions are obtained at equal flow rates from the organic and aqueous phases ($Q_c = Q_d = 28$ L/h) and the maximum pulse intensity (Af = 4.4 cm/s) in which the volumetric mass transfer coefficient is equal to 0.00639 1/s $K_{od} \times a$, and the extraction efficiency is equivalent to 93.34%. The models' evaluation showed that the error of the forward mixing model is less than other models in predicting the results. Deformation of the concentration profile inside the column by examining the effect of pulse intensity (Af) and flow rate ratio (Q_c/Q_d) showed that reducing in the driving force and achieving equilibrium are the effects of the pulsed condition and the increment in continuous phase flow rate. These parameters help to exchange and transfer more ions between both phases with a higher extraction efficiency.
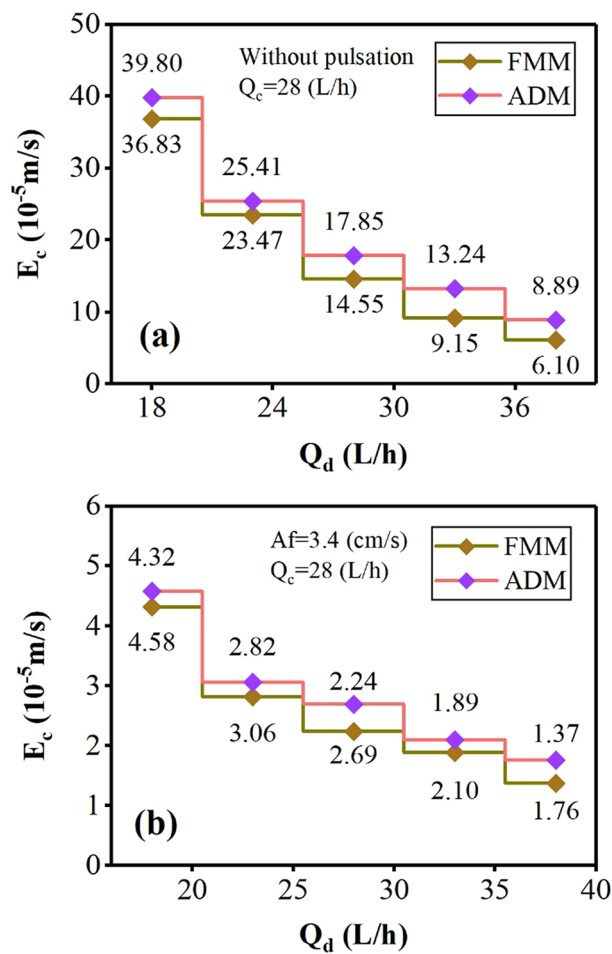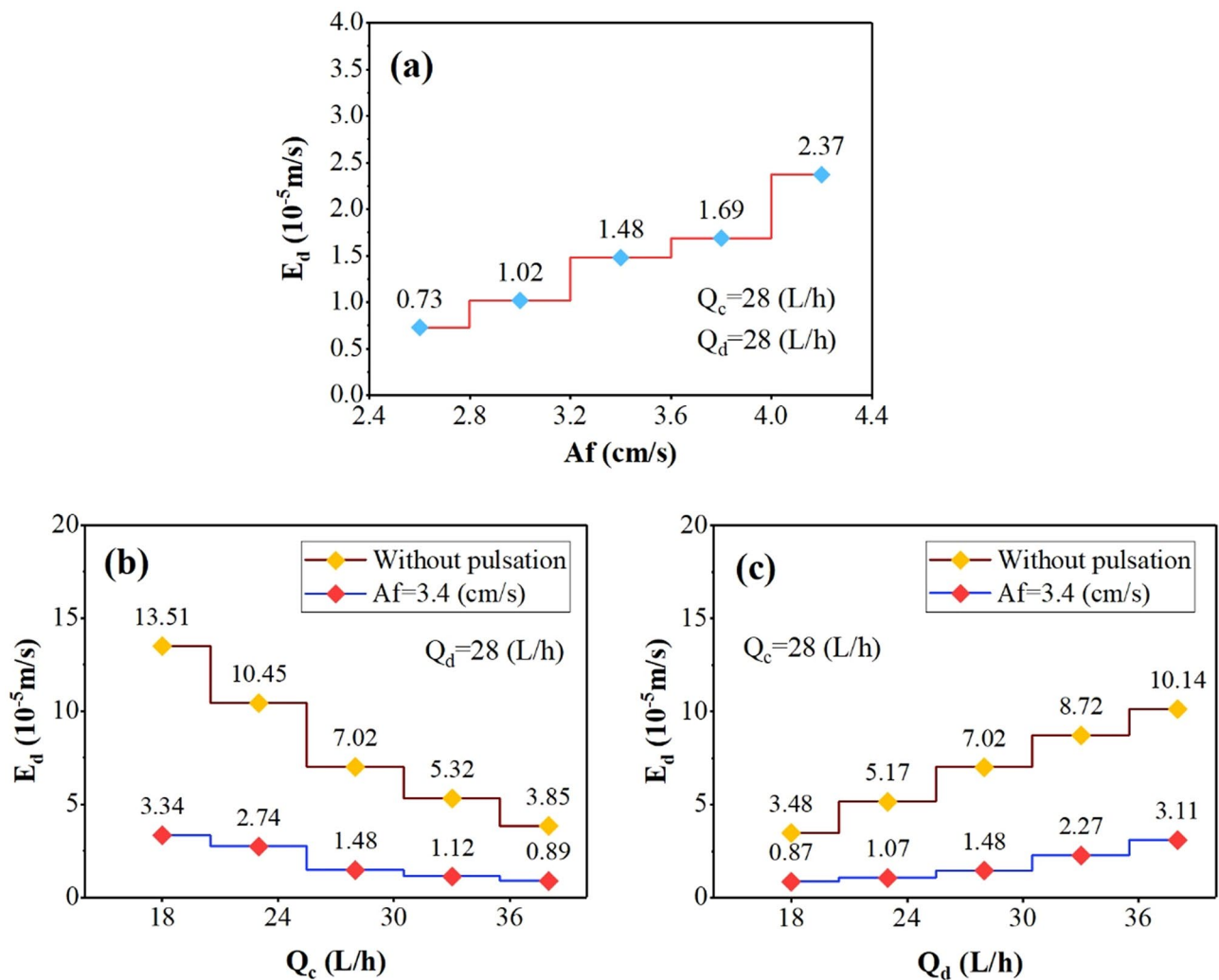
Figure 9. The effect of organic phase flow rate on the continuous phase axial dispersion coefficient (**a**) without pulsation, (**b**) Af = 3.4 (cm/s).

Figure 10. The effect of operating parameters [(**a**) pulsation intensity, (**b**) aqueous phase flow rate, and (**c**) organic phase flow rate] on the dispersed phase axial dispersion coefficient.
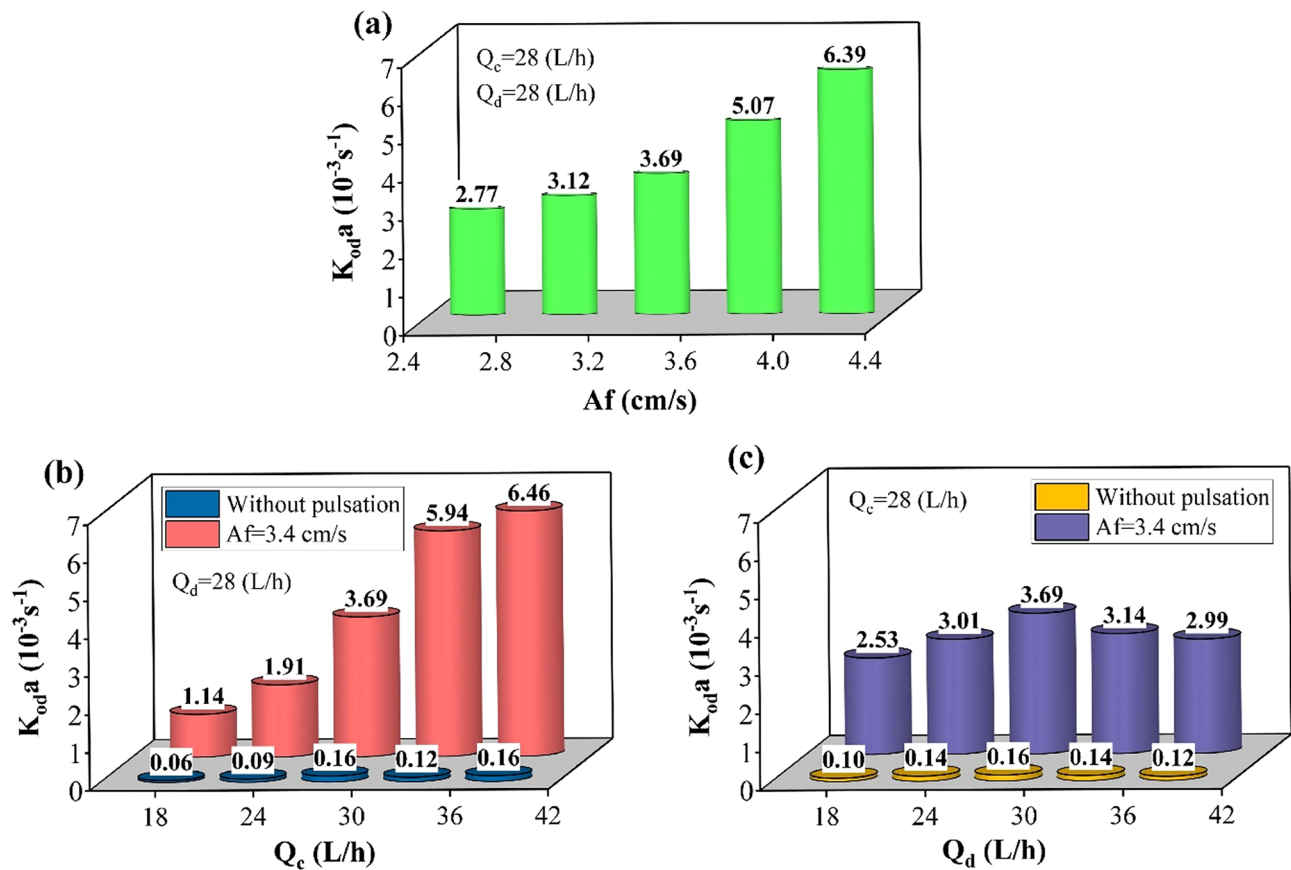
Figure 11. The effect of operating parameters [(**a**) pulsation intensity, (**b**) aqueous phase flow rate, and (**c**) organic phase flow rate] on the volumetric overall mass transfer coefficient predicted by FMM.
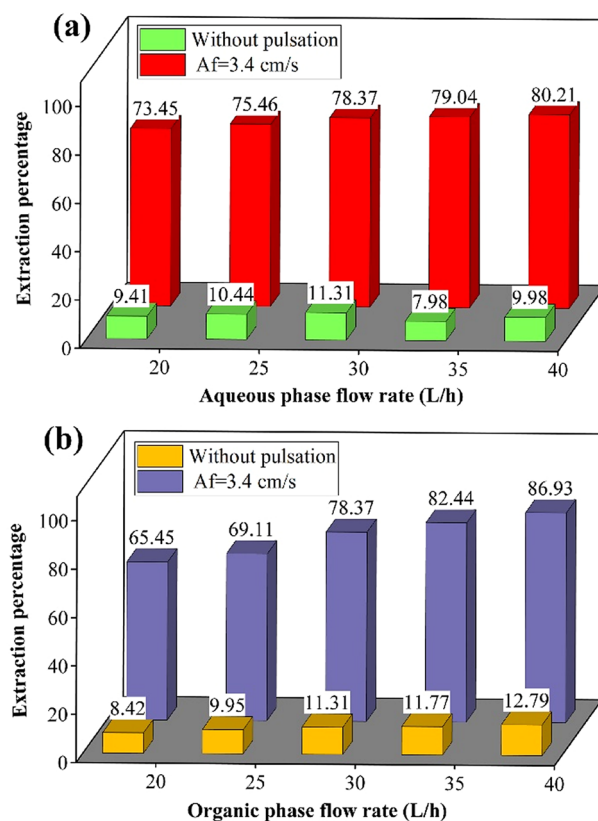
Figure 12. The influence of aqueous and organic phase flow rate on the extraction percentage.

References

1. Torab-Mostaedi, M., Ghaemi, A. & Asadollahzadeh, M. Flooding and drop size in a pulsed disc and doughnut extraction column. *Chem. Eng. Res. Des.* **89**(12), 2742–2751 (2011).
2. Torab-Mostaedi, M., Ghaemi, A., Asadollahzadeh, M. & Pejmanzad, P. Mass transfer performance in pulsed disc and doughnut extraction columns. *Braz. J. Chem. Eng.* **28**, 447–456 (2011).
3. Torkaman, R., Safdari, J., Torab-Mostaedi, M., Moosavian, M. & Asadollahzadeh, M. Extraction of samarium and gadolinium from aqueous nitrate solution with D2EHPA in a pulsed disc and doughnut column. *J. Taiw. Ins. Chem. Eng.* **48**, 18–25 (2015).
4. Shakib, B., Torkaman, R., Torab-Mostaedi, M. & Asadollahzadeh, M. The performance of pulsed scale-up column for permeable of selenium and tellurium ions to organic phase, case study: Disc and doughnut structure. *Chem. Eng. Process.* **157**, 108042 (2020).
5. Liu, J.-Q., Li, S.-W., Wang, Y.-Y., Zhang, Q. & Jing, S. Extraction of uranium nitrate with 30%(v/v) tributyl phosphate in kerosene in a pilot annular pulsed disc-and-doughnut column—Part II: Axial mixing and mass transfer performance. *Solvent Extr. Ion Exch.* **35**(3), 187–198 (2017).
6. Asadollahzadeh, M., Torkaman, R. & Torab-Mostaedi, M. Optimization of lanthanum extraction in asymmetric rotation pilot plant column by using central composite methodology. *Geosystem. Eng.* https://doi.org/10.1080/12269328.2020.1719905 (2020).
7. Asadollahzadeh, M., Torkaman, R. & Torab-Mostaedi, M. Continuous extraction of Europium(III) by ionic liquid in the rotating disk column with an asymmetrical structure aimed at the evaluation of reactive mass transfer. *ACS Omega* **5**(30), 18700–18709 (2020).
8. Dana, M., Shahhosseini, S., Sobati, M. A., Ansari, A. R. & Asadollahzadeh, M. Optimization of extractive desulfurization of diesel oil in a continuous oldshue-rushton column pilot plant. *Energy Fuels* **34**(1), 1041–1052 (2020).
9. Shakib, B., Torab-Mostaedi, M., Outokesh, M. & Asadollahzadeh, M. Direct extraction of Mo(VI) from sulfate solution by synergistic extractants in the rotation column. *Chin. J. Chem. Eng.* https://doi.org/10.1016/j.cjche.2019.11.011 (2020).
10. Ishfaq, A., Ilyas, S., Yaseen, A. & Farhan, M. Hydrometallurgical valorization of chromium, iron, and zinc from an electroplating effluent. *Sep. Purif. Technol.* **209**, 964–971 (2019).
11. Ugwu, E. I. & Agunwamba, J. C. A review on the applicability of activated carbon derived from plant biomass in adsorption of chromium, copper, and zinc from industrial wastewater. *Environ. Monitor. Assess.* **192**, 240 (2020).
12. Song, J. *et al.* A critical review on membrane extraction with improved stability: Potential application for recycling metals from city mine. *Desalination* **440**, 18–38 (2018).
13. Asadollahzadeh, M., Torkaman, R., Torab-Mostaedi, M. & Hemmati, A. Enhancing cerium recovery from leaching solution of glass polishing powder waste using imidazolium ionic liquid. *Waste Biomass Valori.* https://doi.org/10.1007/s12649-020-01070-w (2020).
14. Asadollahzadeh, M., Torkaman, R. & Torab-Mostaedi, M. Recovery of yttrium ions from fluorescent lamp waste through supported ionic liquid membrane: process optimisation via response surface methodology. *Int. J. Environ. Anal. Chem.* https://doi.org/10.1080/03067319.2020.1763976 (2020).
15. Wieszczycka, K., Filipowiak, K., Wojciechowska, I. & Aksamitowski, P. Novel ionic liquid-modified polymers for highly effective adsorption of heavy metals ions. *Sep. Purif. Technol.* **236**, 116313 (2020).

16. Foong, C. Y., Wirzal, M. D. H. & Bustam, M. A. A review on nanofibers membrane with amino-based ionic liquid for heavy metal removal. *J. Mol. Liq.* **297**, 111793 (2020).
17. Tang, J., Petranikova, M., Ekberg, C. & Steenari, B.-M. Mixer-settler system for the recovery of copper and zinc from MSWI fly ash leachates: An evaluation of a hydrometallurgical process. *J. Clean. Prod.* **148**, 595–605 (2017).
18. Hou, J. *et al.* Toxic effects of different types of zinc oxide nanoparticles on algae, plants, invertebrates, vertebrates and microorganisms. *Chemosphere* **193**, 852–860 (2018).
19. Batayneh, A. T. Toxic (aluminum, beryllium, boron, chromium and zinc) in groundwater: Health risk assessment. *Int. J. Environ. Sci. Technol.* **9**, 153–162 (2012).
20. Jafari, H., Abdollahi, H., Gharabaghi, M. & Balesini, A. A. Solvent extraction of zinc from synthetic Zn–Cd–Mn chloride solution using D2EHPA: Optimization and thermodynamic studies. *Sep. Purif. Technol.* **197**, 210–219 (2018).
21. Shah, K., Gupta, K. & Sengupta, B. Selective separation of copper and zinc from spent chloride brass pickle liquors using solvent extraction and metal recovery by precipitation-stripping. *J. Environ. Chem. Eng.* **5**(5), 5260–5269 (2017).
22. Singh, R., Mahandra, H. & Gupta, B. Solvent extraction studies on cadmium and zinc using Cyphos IL 102 and recovery of zinc from zinc-plating mud. *Hydrometallurgy* **172**, 11–18 (2017).
23. Ding, K. *et al.* Efficiently enriching zinc(II) from and into ammonium chloride media with species regulation and Aliquat336. *Sep. Purif. Technol.* **190**, 100–107 (2018).
24. Sun, Q. *et al.* Separation and recovery of heavy metals from concentrated smelting wastewater by synergistic solvent extraction using a mixture of 2-hydroxy-5-nonylacetophenone oxime and bis(2,4,4-trimethylpentyl) -phosphinic acid. *Solvent Ext. Ion Exch.* **36**(2), 175–190 (2018).
25. Song, S. *et al.* Recovery of cobalt and zinc from the leaching solution of zinc smelting slag. *J. Environ. Chem. Eng.* **7**, 102777 (2019).
26. Shakib, B., Torkaman, R., Torab-Mostaedi, M. & Asadollahzadeh, M. Mass transfer studies in RDC column by the coupling effects of perforated structure and reactive extraction of Mo(VI) and W(VI) from sulfate solution. *Int. Commun. Heat Mass Trans.* **118**, 104903 (2020).
27. Torab-Mostaedi, M., Ghaemi, A. & Asadollahzadeh, M. Prediction of mass transfer coefficients in a pulsed disc and doughnut extraction column. *Can. J. Chem. Eng.* **90**(6), 1570–1578 (2012).
28. Hemmati, A., Torab-Mostaedi, M. & Asadollahzadeh, A. Mass transfer coefficients in a Kühni extraction column. *Chem. Eng. Res. Des.* **93**, 747–754 (2015).
29. Torab-Mostaedi, M. & Asadollahzadeh, M. Mass transfer performance in an asymmetric rotating disc contactor. *Chem. Eng. Res. Des.* **94**, 90–97 (2015).
30. Asadollahzadeh, M. *et al.* Use of axial dispersion model for determination of Sherwood number and mass transfer coefficients in a perforated rotating disc contactor. *Chin. J. Chem. Eng.* **25**(1), 53–61 (2017).
31. Thornton, J. D. *Science and Practice of Liquid–Liquid Extraction* (Oxford University Press, 1992).
32. Asadollahzadeh, M., Shahhosseini, S., Torab-Mostaedi, M. & Ghaemi, A. Mass transfer performance in an Oldshue-Rushton column extractor. *Chem. Eng. Res. Des.* **100**, 104–112 (2015).
33. Torab-Mostaedi, M., Asadollahzadeh, M. & Safdari, J. Prediction of mass transfer coefficients in an asymmetric rotating disk contactor using effective diffusivity. *Chin. J. Chem. Eng.* **25**(3), 288–293 (2017).
34. Lo, T. C., Commercial liquid–liquid extraction equipment. In *Handbook of Separation Techniques for Chemical Engineers*, Schweitzer, P. A., Ed. McGraw-Hill, 1979.
35. Asadollahzadeh, M., Torab-Mostaedi, M., Shahhosseini, S. & Ghaemi, A. Holdup, characteristic velocity and slip velocity between two phases in a multi-impeller column for high/medium/low interfacial tension systems. *Chem. Eng. Process.* **100**, 65–78 (2016).
36. Asadollahzadeh, M., Torab-Mostaedi, M., Shahhosseini, S., Ghaemi, A. & Torkaman, R. Unified new correlation for prediction of dispersed phase holdup in agitated extraction columns. *Sep. Purif. Technol.* **158**, 275–285 (2016).
37. Korchinsky, W. J. & Young, C.-H. Computational techniques for liquid–liquid extraction column model parameter estimation, using the forward mixing model. *J. Chem. Technol. Biotechnol.* **35A**, 66 (1985).
38. Korchinsky, W. J. & Bastani, D. Application of 'forward mixing' model to the low interfacial tension system n-butanol—succinic acid—water in rotating disc contactor liquid extraction columns. *J. Chem. Technol. Biotechnol.* **58**(2), 113–122 (1993).
39. Liu, J.-L. & Xia, R. A unified analysis of a micro-beam, droplet and CNT ring adhered on a substrate: Calculation of variation with movable boundaries. *Acta. Mech. Sin.* **29**(1), 69–72 (2013).
40. Torab-Mostaedi, M., Ghaemi, A., Asadollahzadeh, M. & Pejmanzad, P. Mass transfer performance in pulsed disc and doughnut extraction columns. *Braz. J. Chem. Eng.* **28**(3), 447–456 (2011).
41. Wang, Y., Yi, H., Smith, K., Mumford, K. & Stevens, G. Mass transfer in a pulsed and non-pulsed disc and doughnut (PDD) solvent extraction column. *Chem. Eng. Sci.* **165**, 48–54 (2017).
42. Wang, Y., Yi, H., Smith, K. H., Mumford, K. A. & Stevens, G. W. Axial dispersion in a pulsed and nonpulsed disc and doughnut solvent extraction column. *Ind. Eng. Chem. Res.* **56**(14), 4052–4059 (2017).
43. Yi, H., Wang, Y., Smith, K. H., Fei, W. & Stevens, G. W. Hydrodynamic performance of a pulsed solvent extraction column with novel ceramic internals: Holdup and drop size. *Chem. J.* **56**(4), 999–1007 (2017).
44. Torkaman, R., Safdari, J., Torab-Mostaedi, M., Moosavian, M. A. & Asadollahzadeh, M. Extraction of samarium and gadolinium from aqueous nitrate solution with D2EHPA in a pulsed disc and doughnut column. *J. Taiw. Int. Chem. Eng.* **48**, 18–25 (2015).
45. Ferreira, A. E. *et al.* Extraction of copper from acidic leach solution with Acorga M5640 using a pulsed sieve plate column. *Hydrometallurgy* **104**(1), 66–75 (2010).
46. Gameiro, M. L. F., Machado, R. M., Ismael, M. R. C., Reis, M. T. A. & Carvalho, J. M. R. Copper extraction from ammoniacal medium in a pulsed sieve-plate column with LIX 84-I. *Hazard. Mater.* **183**, 165–175 (2010).

Author contributions

M.A. and M.T.-M. wrote the main manuscript text and M.S. and R.T. prepared figures. All authors reviewed the manuscript.

Competing interests

The authors declare no competing interests.

Additional information

Correspondence and requests for materials should be addressed to M.A.

Reprints and permissions information is available at www.nature.com/reprints.

Publisher's note Springer Nature remains neutral with regard to jurisdictional claims in published maps and institutional affiliations.